16th ICAAR LISBOA 2020-2022

16th International Conference on
Alkali-Aggregate Reaction in Concrete
Lisboa | LNEC | Portugal | 31 May - 2 June 2022

http://icaar2020-2022.lnec.pt

Influence of different expansion models on the anisotropy of ASR expansion under restraint evaluated by 3D-RBSM

Taito Miura [(1)], Stephane Multon [(2)], Yuichiro Kawabata [(3)]

(1) *Department of Civil Engineering, Nagoya University, Nagoya, Japan, t.miura@civil.nagoya-u.ac.jp*

(2) LMDC, Université de Toulouse, INSA/UPS Génie Civil, Toulouse, France, multon@insa-toulouse.fr

(3) Port and Airport Research Institute, Yokosuka, Japan, kawabata-y@p.mpat.go.jp

Abstract

In this study, the effect of different aggregate types on the expansion behavior under restraint stress is assessed. In the analysis, a three-dimensional rigid body spring model (3D-RBSM) is used with an aggregate model in which concrete is explicitly modeled as coarse aggregates and mortar, and the expansion phase inside the aggregates is randomly placed on the basis of two expansive site models: the gel pocket model (GPM) proposed by Dunant et al. (2010) and reaction rim model (RRM) proposed by Ichikawa et al. (2007). The imposed strain is input to the expansion phase to express the expansion behaviors of aggregates for these models. The analysis is based on the experiment of alkali silica reaction (ASR) under constraint performed by Multon et al. (2006), in which expansion transfer was confirmed. In the first analysis, the analytical parameters are identified to reproduce free expansion. In particular, a model in which expansion stops after a certain expansion period (the expansion stop model) and a model in which expansion pressure dissipates after a certain crack width (the crack effect model) are constructed to represent the plateau of the expansion. By using these models to reproduce free expansion, the expansion behaviors under the uniaxial loadings of 5, 10, and 20 MPa are evaluated. The results confirm that the present analysis can evaluate the expansion behavior under loadings of up to 10 MPa without divergence in the numerical analysis. Regarding the difference in the expansion behavior between the expansion stop model and the crack effect model, it is confirmed that the expansion transfer could not be reproduced in the expansion stop model while it is shown only in the crack effect model with the RRM.

Keywords: *aggregate type, anisotropy, alkali silica reaction, expansion, 3D-RBSM*

1. INTRODUCTION

Alkali silica reaction (ASR) causes expansion cracks in aggregate and cement paste. Reactive silica dissolved in high-pH solution of aggregate paste forms ASR gel. When the ASR gel comes in contact with the cement paste, alkalis in the gel tend to be exchanged with Ca to form C-S-H gel [1]. The expansion mechanisms of ASR and the generation and propagation processes of expansion cracks are not yet fully understood although some mechanisms have been proposed [1-4]. In massive concrete structures such as dams, the self-weight of the structure and the restraint stress caused by boundary conditions lead to anisotropy of expansion; that is, the expansion in a direction perpendicular to the restraint stress is different from free expansion. However, some researchers [5, 6] observed a controversial phenomenon of expansion transfer by which the expansion in a direction perpendicular to the restraint stress is larger than free expansion, while others [7] could not observe such transfer. Moreover, the trend of reduction in mechanical properties under restrained expansion conditions has been reported to differ from that under free expansion as there exists a directionality of the internal crack under restraint stress [8]. Therefore, direct application of the relationship between mechanical properties and expansion obtained in stress-free conditions to expansion under a restraint condition may not be feasible. Furthermore, the anisotropy of expansion complicates the assessment of deformation performance of existing structures.

The internal cracks under free expansion appear in the sharp crack or onion skin crack pattern [9]. Our previous numerical investigation [10] indicated that the crack pattern strongly depends on the distribution of the expansive site where the expansion pressure inside aggregates accumulates. Furthermore, the sharp crack and onion skin crack can be explained by the gel pocket model (GPM) [7] and reaction rim model (RRM) [3], respectively. The changes in the internal crack pattern with the distribution of the

expansive sites in aggregates may in turn affect the crack propagation process and stress resisting mechanism at the cross-sectional area under the restraint condition.

This study conducted a numerical analysis to clarify the effect of the distribution of expansive sites on the anisotropy of ASR expansion under stress. Using the mesoscale discrete model, namely the three-dimensional rigid body spring model (3D-RBSM), which can explicitly describe coarse aggregates and mortar, the expansion behaviors at different expansive sites under several stress conditions were assessed. The results were compared with those of the laboratory experiments performed by Multon et al. [5].

2. OVERVIEW OF MESOSCALE DISCRETE ANALYSIS

In this study, the anisotropy of ASR expansion was numerically investigated by the 3D-RBSM with an aggregate model that can describe the different distributions of the expansive sites in the aggregate. The two different internal crack patterns have been explained by the difference in the expansive sites by using the expansive site models GPM and RRM [10]. In this analysis, to reproduce the time-dependent behaviors of ASR expansion, a creep model and two expansion pressure models were applied. The analytical parameters of the expansive site model and expansion pressure model were calibrated on the expansion data obtained from Multon et al. [5] and applied to the expansion under various stresses. The details of the analysis are described in the subsequent sections.

2.1 3D Rigid Body Spring Model

The 3D-RBSM is a discrete model proposed by Kawai [11] and used for describing cracks. It is composed of rigid body elements discretized using random Voronoi particles and mechanical springs allocated between the particles as shown in Figure 2.1. The mechanical springs comprise one normal spring and two shear springs arranged at integral points on the boundary surface. The tensile, compressive, and shear constitutive laws are shown in Figure 2.2. The mesoscale parameters for the mesoscale constitutive law introduced to the normal and shear springs are listed in Table 2.1. Further details on the model are provided in [10].

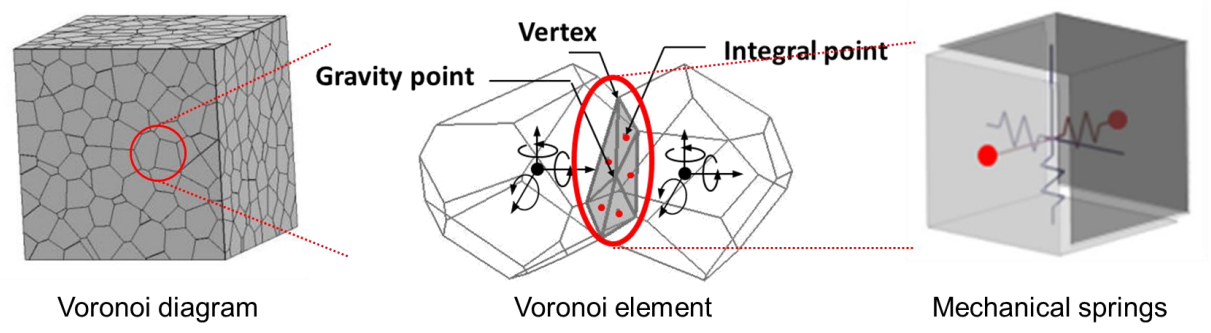

Figure 2.1 3D rigid body spring model

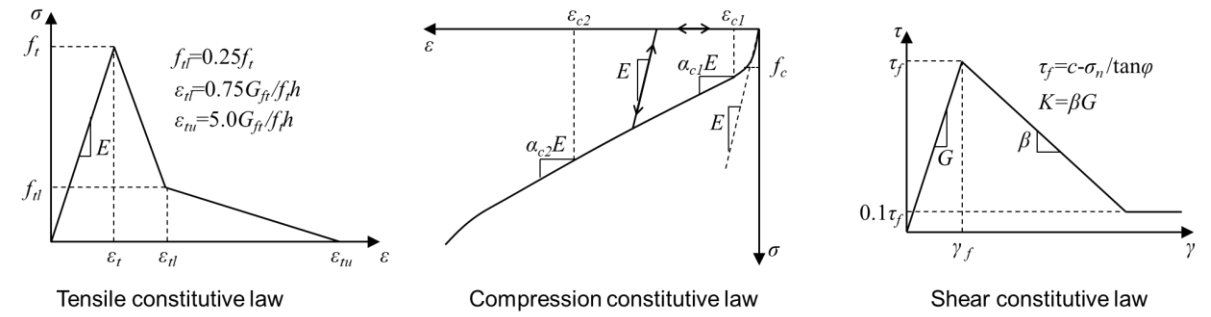

Figure 2.2 Mesoscale constitutive models for normal and shear springs

Table 2.1 Mesoscale parameters of the mesoscale constitutive law for the mechanical springs.

NORMAL SPRING							
Elastic modulus	Tensile constitutive law		Compressive constitutive law				
E (MPa)	σ_t (MPa)	g_f (N/mm)	f'_c (MPa)	ε_{c1}	ε_{c2}	α_{c1}	α_{c2}
1.4 E^*	0.8 f_t^*	0.5 G_f^*	1.5 f'^*_c	$-2\sigma_c$ $/(E(1+\alpha_{c1}))$	-0.015	0.15	0.25

SHEAR SPRING							
Shear stiffness	Mohr–Coulomb fracture criteria			Softening coefficient			
$\eta = G/E$	c (MPa)	φ	σ_b (MPa)	β_0	β_{max}	X	k
0.35	0.14 f'^*_c	37	f'^*_c	-0.05	-0.02	-0.01	-0.3

* indicates macroscopic mechanical properties.

2.2 Aggregate model

An aggregate model represents multiple spherical aggregates randomly arranged in the analytical model. The analytical model is a cube of dimensions 130 × 130 × 130 mm consisting of 90 randomly placed coarse aggregates, each having a diameter of 20 mm. The average element size in the aggregate particles was 1 mm and the maximum mortar element size was 3 mm. In this analysis, three analytical models were constructed to consider the variation in the expansion behavior depending on the arrangement of aggregates.

The material properties of mortar, aggregate, and ITZ (Interfacial Transition Zone) are indicated in Table 2.2, and further details can be seen in [10].

Table 2.2 Material properties for the mortar and aggregates

	fc' (MPa)	E (GPa)	f_t (MPa)	c (MPa)	G_f (Nm)
Aggregate	150.0	70.0	8.80	14.0	0.0005
Mortar	52.5	41.3	1.97	4.9	0.0280
ITZ	26.25	20.65	0.98	2.45	0.0140

2.3 Expansive site model

The GPM proposed by Dunant et al. [7] and the RRM proposed by Ichikawa et al. [3] were used as expansive site models. These models assumed that the sites where the imposed strain is applied do not change during expansion even after cracking.

The GPM and RRM analytical models are indicated in Figure 2.3. For the GPM, the elements containing expansive sites were randomly selected in the aggregate elements. The expansive site ratio with respect to the entire aggregate elements was set to 1.0%.

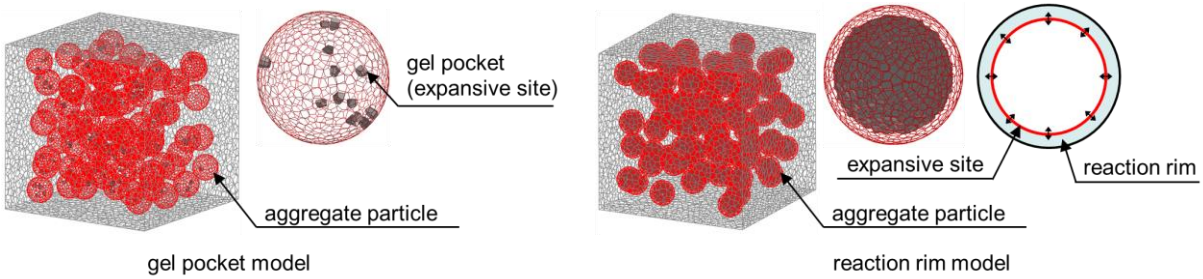

Figure 2.3 Expansive site models (left: gel pocket model, right: reaction rim model)

For the RRM, the expansive sites are considered to form at the inner area of the reaction rim. The location of the expansion pressure inside the aggregate is likely a very thin layer. Based on the previous study [10], this study used the boundary model in which the thin expansive sites are localized at the inner surface of the reaction rim. The thickness of the reaction rim was assumed to be 2 mm based on Ichikawa et al. [3].

2.4 Expansion pressure model

To consider the plateau of the expansion, two different assumptions were made for the expansion models.

First, it was supposed that the expansion stops with the completion of the reaction of the ASR gel (i.e., the expansion stop model). Second, it was assumed that the expansion pressure is dissipated by the flow of the ASR gel into the induced cracks with decreasing pressure (i.e., the crack effect model). For the expansion stop model, the time when expansion stopped was set for reproducing free expansion. For the crack effect model, the strain was imposed on the expansive site before a crack reaches the threshold crack width, and the imposed strain increase was set to zero when the crack width exceeded the threshold (as shown in Figure 2.4). As several crack width thresholds were applied for the calibration, the optimum crack width threshold was determined to fit the free expansion. This analysis neglected other factors influencing the expansion, such as relative humidity, thereby focusing only on the mechanical properties.

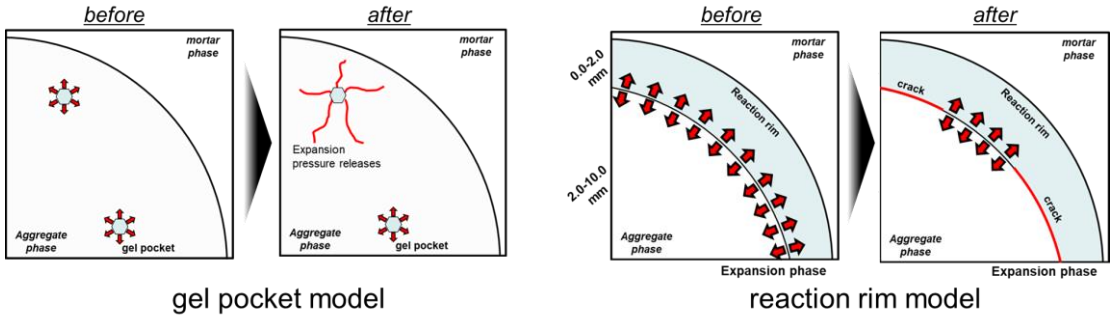

Figure 2.4 Crack effect model (left: GPM, right: RRM)

2.5 Creep model

To consider the time-dependent behavior of cementitious materials, a creep model was applied. The creep model was developed on the basis of the JSCE model [12] with a small modification to apply it to the mesoscale discrete analysis. The modified creep model is expressed as follows.

$$\varepsilon_{i,t} = \alpha \sum_{tj=0}^{t} \Delta\sigma_{i,tj} \cdot \frac{4W(1-RH)+350}{12+f_c'} \cdot log\left(t-t_j+1\right) \cdot 10^{-6} \quad (1)$$

where $\varepsilon_{i,t}$ is the total creep strain, α is the mesoscale coefficient, $\Delta\sigma_{i,tj}$ is the increment stress from t_{-1} to t, W is the water content per unit (kg/m^3), RH is the relative humidity, and f_c' is the compressive strength (MPa).

Creep strain calculated step-by-step method using the modified creep model was applied to normal and shear springs of only the mortar phases in the same manner. When the original JSCE creep model is applied, the effect of creep tends to be considerably large. Therefore, the mesoscale coefficient α was applied to reduce the effect of creep. The mesoscale coefficient α was determined by sensitivity analysis to fit the macroscopic deformation of specimens under restraint stress with no expansion.

2.6 Restraint condition

In the numerical analysis, the restraint condition was described by the stresses applied in the y-direction to the restraint plates located at the top and bottom surfaces of the analytical model. The stresses were set at 5, 10, and 20 MPa. In the laboratory experiment, the friction between the restraint plates and the

specimen was not removed. The objective of the analysis was the middle of the specimen, which was probably little influenced by the friction, and the friction between the restraint plates and the analytical model was, therefore, removed in this analysis. The definition of macroscopic expansion is shown in Figure 2.5.

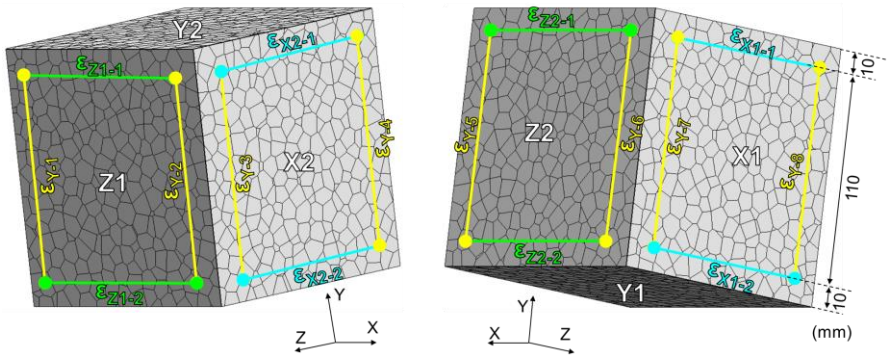

Figure 2.5 Definition of macroscopic expansion

3. ANALYTICAL RESULTS

3.1 Sensitivity analysis for reproducing free expansion

To set the analytical parameters to reproduce the ASR expansion, sensitivity analyses were carried out on the laboratory experiment performed by Multon et al. [5]. The mesoscale coefficient α of the modified creep model was determined from the deformation change under various stresses with the data obtained on specimens with no expansion. In addition, the analytical parameters for the expansion pressure model were defined by the data obtained for specimens submitted to free expansion.

3.1.1 Effect of creep

The reproducibility of the creep behavior under various stresses was verified by fitting the mesoscale coefficient α as shown in Figure 3.1. When the coefficient was set to 1.0 (equivalent to that of the JSCE creep model), the creep effect was considerably large. As the coefficient decreased, the creep effect reduced. It was confirmed that the creep behavior under all restraint stresses can be reproduced at α = 0.55. The original JSCE creep model is a macroscopic phenomenological model constructed using the data of numerous concrete materials. It cannot be directly applied to mesoscale discrete analysis. When aggregates are explicitly meshed, the creep strain is concentrated in the cement paste (or in the mortar if the aggregates are not meshed). The JSCE model has not been designed for this use. Moreover, the normal and shear springs of the 3D-RBSM represent the response of concrete under normal and shear stress, respectively. Because concrete creep under normal and shear loading differs, different creep models are required for normal and shear springs. Nevertheless, the modified creep model can describe the deformation behavior under various stresses while not considering these factors. Hence, in this study, the modified creep model was applied to the ASR expansion analysis under free and restraint conditions. Thus, the effect of the time-dependent behavior of concrete on the damage induced by ASR is partly considered.

3.1.2 Expansion stop model

In the expansion stop model, the plateau of the expansion was considered by setting the time when the expansion stops. The imposed strain and the stop time were calibrated on the data under free expansion obtained from the experiment. The optimum imposed strains to describe the free expansion for the GPM and RRM were 75 and 25 μm/m/day, respectively. Note that the imposed strain is one of the analytical parameters. The stop time of expansion was set to 250 days for both expansive site models because the expansion plateau was reached after approximately 250 days in the experiment. Figure 3.2 shows the comparison of the free expansion calculated by the GPM and RRM with the experimental results. It can be confirmed that the analytical result can reproduce the experiment.

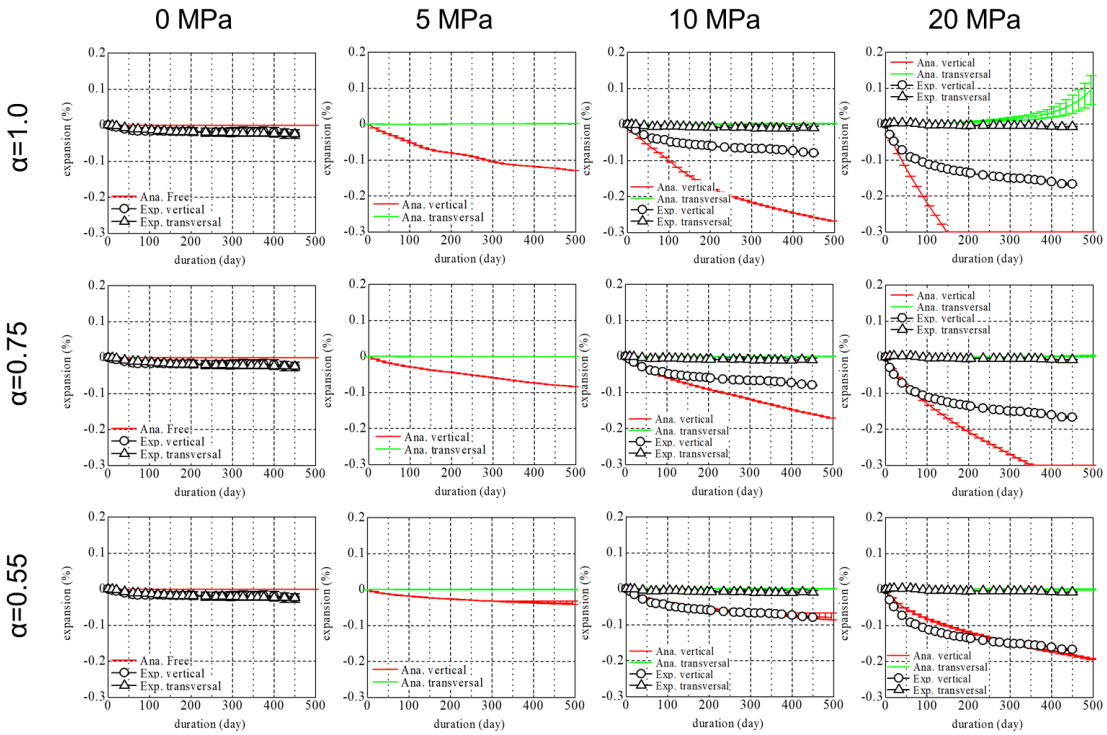

Figure 3.1 Sensitivity analysis of the creep model with the no-expansion specimen for mesoscale coefficients α = 1.0, 0.75, and 0.55.

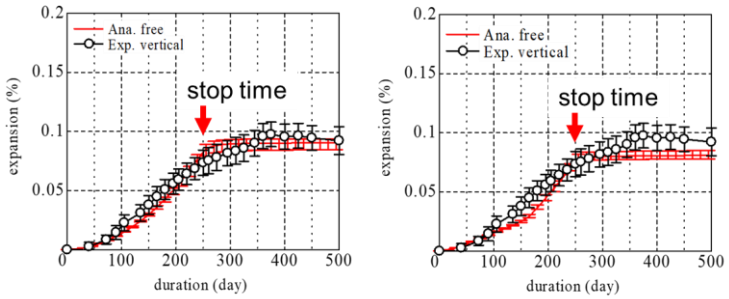

(a) gel pocket model (b) reaction rim model

Figure 3.2 Free expansion calculated by the GPM and RRM with the expansion stop model in comparison with experimental results

3.1.3 Crack effect model

The crack effect model reproduces the plateau of expansion by providing no additional imposed strain when the crack width reaches the threshold. The threshold of crack width is defined as the width of the crack when the ASR gel starts to flow into the crack. The imposed strain is the same as that in the expansion stop model because it is determined by the initial stage of expansion before crack formation. The crack width thresholds were set to 0.01, 0.03, and 0.05 mm for the GPM and 0.005, 0.01, and 0.05 mm for the RRM. In addition, the case with no crack effects was also analyzed for comparison.

Figure 3.3 indicates the results of the sensitivity analysis for the crack width threshold in the GPM and RRM. When the crack width reached the threshold, the evolution of the expansion rate decreased at a certain time and the expansion gradually plateaued. The trends of the starting time and the decrease of the expansion evolution rate decreased with the higher crack width threshold. The optimum thresholds of crack width in the GPM and RRM were 0.03 and 0.01 mm, respectively.

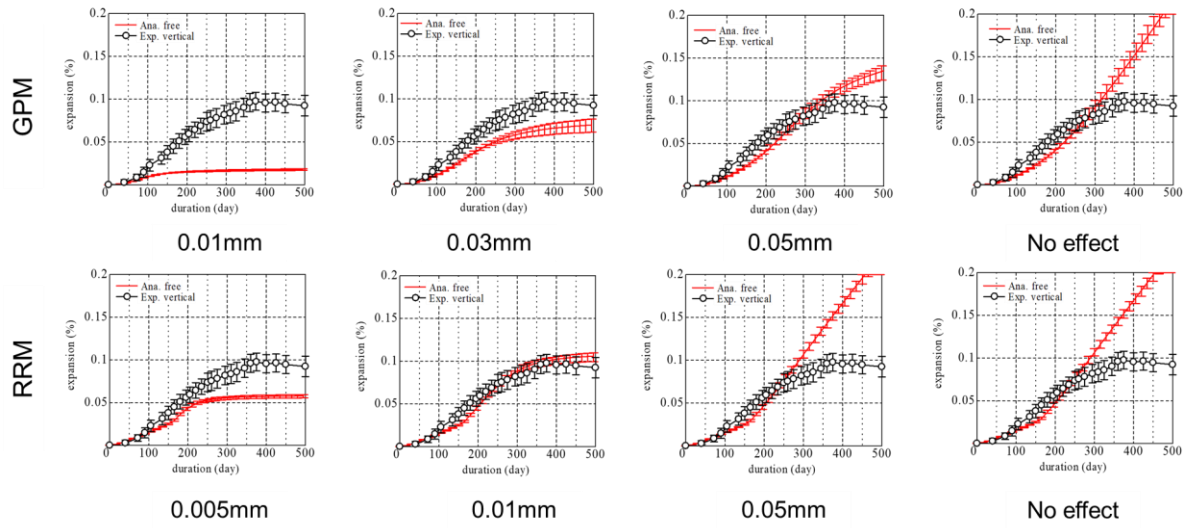

Figure 3.3 Sensitivity analysis for the threshold of crack width of the crack effect model with the GPM and RRM

In the two expansion pressure models analyzed in this study, the expansion plateau was reproduced by the completion of the generation of ASR gel by chemical reactions in the case of the expansion stop model or by the dissipation of expansion pressure due to the flow of the ASR gel to into cracks in the case of the crack effect model. In reality, these models cannot completely reproduce all the actual phenomena. Kawabata et al. [4] observed that the uptake of Ca by the ASR gel can lead to the precipitation of C-S-H gel with low mobility compared to the fresh ASR gel in aggregates that are less viscous and thus flow easily. Such products can close the crack opening and serve as a plug of the system facilitating expansion. The presence of such a plug facilitates another mechanism of expansion to accumulate further expansion pressure owing to the subsequent generation of ASR gel, leading to additional expansion with new crack formation. The current analysis, however, does not fully consider these phenomena. Therefore, the absolute values of the analytical parameters do not precisely have a phenomenological meaning and should be considered as the parameters of the proposed models for the generation and accumulation of expansion pressure in this study.

The analytical parameters are summarized in Table 3.1.

Table 3.1 Analytical parameters

Expansion pressure model	Expansive site model	Mesoscale coefficient for creep	Imposed strain	Stop time	Threshold of crack width
Expansion stop model	GPM	0.55	75 μm/m/day	250day	-
	RRM		25 μm/m/day		-
Crack effect model	GPM		75 μm/m/day	-	0.03 mm
	RRM		25 μm/m/day	-	0.01 mm

3.2 Expansion under restraint

With the analytical parameters determined in the previous section, the expansion under restraint stress was numerically investigated.

3.2.1 Expansion stop model

Figure 3.4 shows the comparison of the expansion under various stresses based on the expansion stop model and the experiment results. The analytical result of 5 MPa stress was taken as a reference result because no experimental data were available for this stress value.

According to these figures, all the calculated transversal expansions were lower than the free expansion while the vertical expansion was similar to the experiment results. For the RRM, the transversal expansion was relatively close to the free expansion, yet always lower than the experiment result. In the experiment, the transversal expansion became larger than the free expansion with the increase in the longitudinal stress [5]. By contrast, the expansion transfer could be observed in the analytical results of both expansive site models.

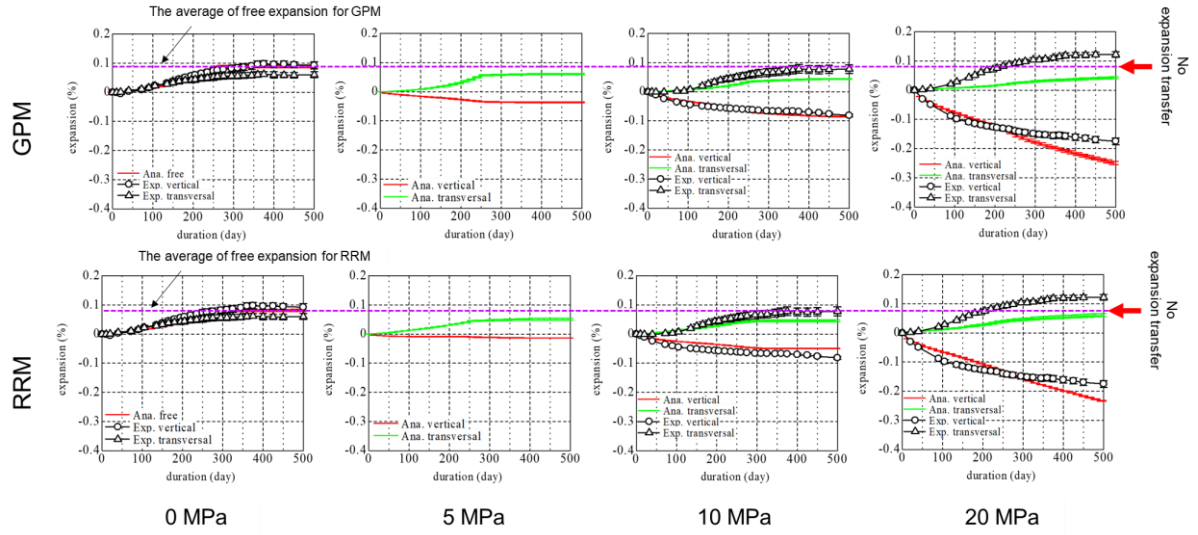

Figure 3.4 Expansion evolution under different stresses calculated by the expansion stop model in the GPM and RRM

3.2.2 Crack effect model

Figure 3.5 shows the comparison of the expansion under various stresses based on the crack effect model and the experiment results.

For the GPM, the resulting expansion was the same as that of the expansion stop model. For the RRM, the transversal expansion under all stress values was slightly larger than the free expansion. This trend is similar to that of expansion transfer. When the restraint stress was 20 MPa, the ultimate expansion was larger than the free expansion, while the time of the start of expansion and the plateau of the

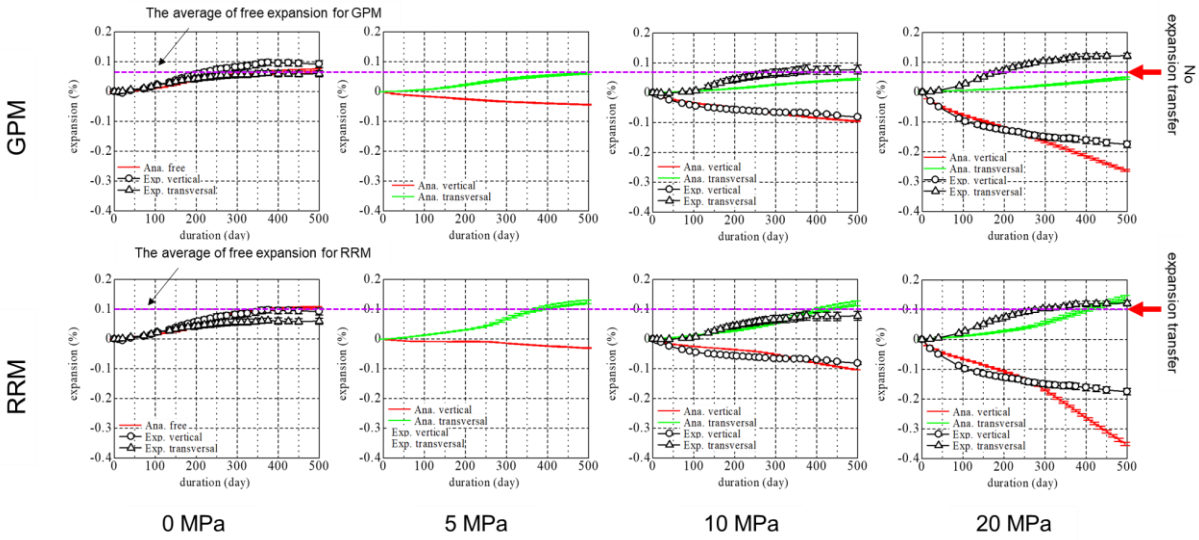

Figure 3.5 Expansion evolution under different stresses calculated by the crack effect model in the GPM and RRM

expansion was delayed. In this case, the vertical strain dramatically decreased from 300 days. Therefore, this analysis can reproduce the anisotropy of expansion under stress of less than 10 MPa while the expansion evolution is slower than the experiment result. This gap between the analytical and experiment results for the 20 MPa loading case can be attributed to the ease of crack formation in the aggregates due to their shape; natural aggregates are not spherical. In addition, due to the heterogeneity of aggregates, the formation of the reaction rim may not be uniformly distributed. The heterogeneity can be the cause of stress concentration at local points. The nonuniform distribution of the stress state in the aggregate probably induces early cracking. Furthermore, creep is an important factor to reproduce the crack propagation process; therefore, the simplified creep model applied to this model may also lead to the gap between the numerical and the experiment results.

4. DISCUSSION

The analytical results suggest the occurrence of expansion transfer in the case of the RRM with the crack effect model. Expansion transfer did not occur in the case of the expansion stop model probably because the imposed strain was zero after 250 days. For the crack effect model, the mechanism of expansion transfer can be discussed in terms of the internal crack and stress distributions. Figures. 4.1 and 4.3 indicate the results of transversal expansions and Figures. 4.2 and 4.4 show the deformation evolution diagrams and internal crack and stress distributions under free expansion and 10 MPa stress calculated by the GPM and RRM, respectively.

For the GPM, according to the deformation variation diagrams shown in Figure 4.2, the surface cracks developed with time and the crack distribution could be observed. By contrast, the density of cracks clearly decreased under the stress condition. For the internal crack distribution in the case of free expansion, the cracks were generated from the expansive sites inside aggregates and gradually propagated to mortar with time. In the case of expansion under stress, the crack generation was delayed, and the cracks propagated only parallel to the loading direction. For the internal stress distribution in the x and y directions under free expansion, compressive stress was accumulated at the expansive sites inside aggregates and tensile stresses acted around the area, generating the compressive stress to ensure stress balance at the cross-sectional area. By contrast, for the internal stress in the y direction in the case of expansion under stress, higher compressive stresses were locally generated at the expansive sites.

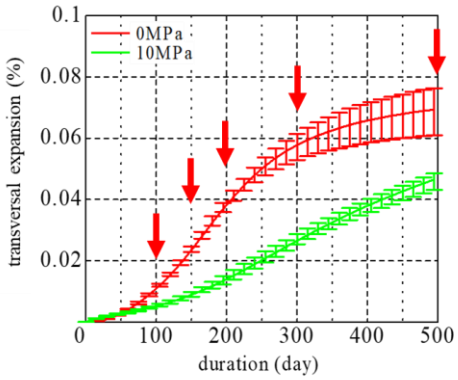

Figure 4.1 Comparison of transversal expansion under 0 and 10 MPa stress calculated by the GPM

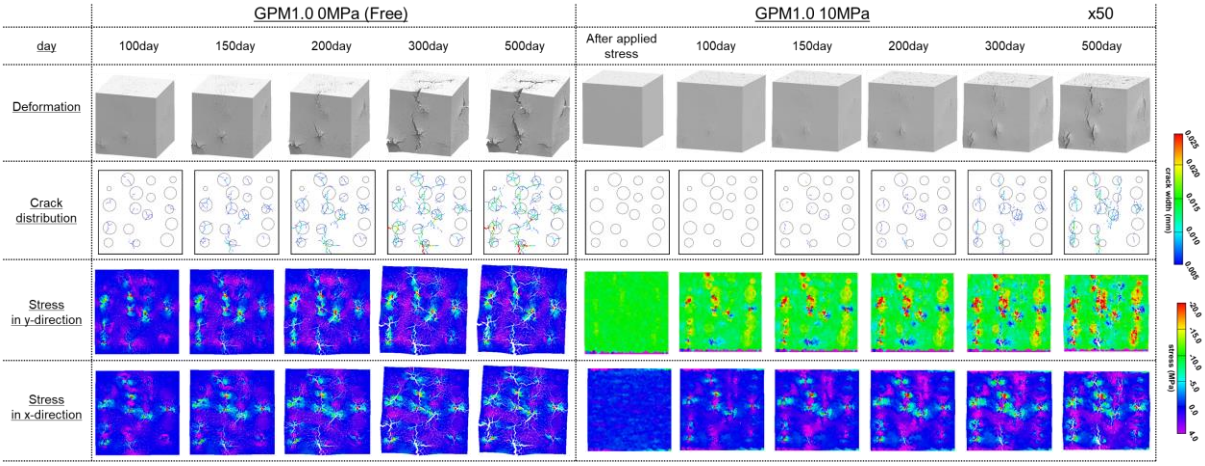

Figure 4.2 Deformation evolution diagram and crack and stress distributions at the cross-sectional area as calculated by the GPM with the crack effect model.

The cracked area at the mortar that could not resist the compressive stress increased with the development of cracks. Consequently, the compressive stress at the expansive sites increased and was distributed randomly inside aggregates. For the internal stress in the x direction, the stress distribution was almost the same as that in case of free expansion, whereas the tensile stress was greater than that in case of free expansion. This tensile stress is important to explain the crack propagation in the vertical direction, and the larger tensile stress accumulation than under free expansion is due to the absence of longitudinal cracks.

In the case of the GPM, the crack directionality may be fixed in advance after the expansive sites were distributed. Therefore, the expansion cracks that were likely to propagate in the transversal direction under free expansion were probably inhibited by the restraint stress, thereby preventing crack propagation in the transversal direction. This may be the reason for the transversal expansion being always smaller than under free expansion.

For the RRM as shown in Figure 4.4, the deformation evolution diagrams were similar to those for the GPM. For the internal crack distribution under free expansion, the cracks generated at the inner surface of the reaction rim after 150 days and gradually propagated and connected with adjacent aggregates. The generation of internal crack distribution under stress was slightly delayed. Numerous expansion cracks appeared after 300 days under free expansion, whereas they were clearly delayed under the stress condition. However, after 500 days, many expansion cracks under the stress condition were generated around the expansive sites inside aggregates and were connected with adjacent aggregates. As shown in the internal stress distribution in the x and y directions in the case of free expansion, the compressive stress was generated at the expansive sites and tensile stress was generated inside aggregates and mortar. The decrease in the tensile stress accompanied with the crack propagation at the aggregates and mortar. For the internal stress in the y direction in the stress condition case, the higher compressive stress inside aggregates could be observed before cracking. As the expansion cracks generated and propagated with time, the compressive stress at the inner area of the reaction rim gradually decreased and the compressive stress around the cracked mortar area also decreased. In comparison to the GPM, the compressive stress inside aggregates was maintained around the reaction rims and was relatively higher. For the internal stress in the x direction, the stress distribution was almost the same as under free expansion. This trend is similar to that of the GPM, while a larger tensile stress was accumulated in the cross-sectional area than in case of the GPM.

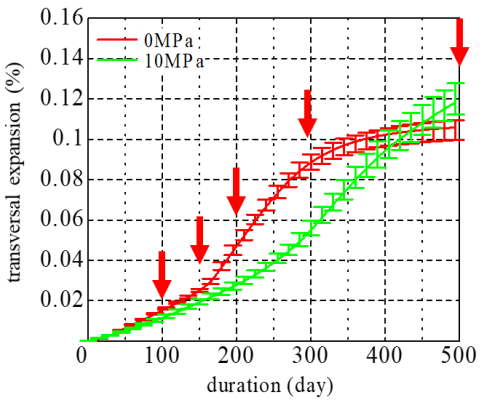

Figure 4.3 Comparison of transversal expansion under 0 and 10 MPa stress calculated by the RRM

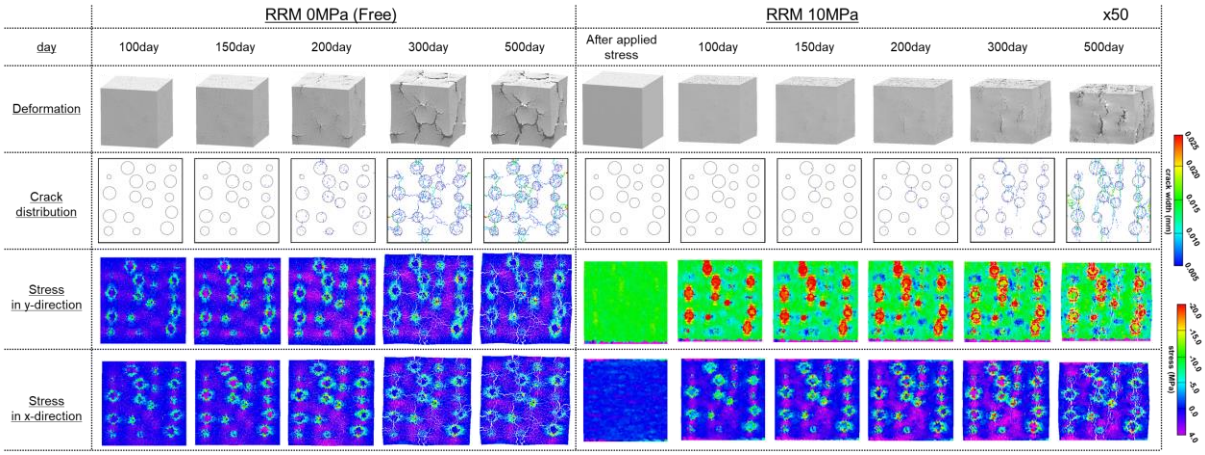

Figure 4.4 Deformation evolution diagram and crack and stress distributions at the cross-sectional area as calculated by the RRM with the crack effect model.

Based on the analytical investigations, a difference of the internal state between the GPM and RRM was the freedom of directionality of expansion cracks. In the case of the GPM, the directionality of a crack was fixed intrinsically owing to the distribution of the expansive sites, which prevents restraint stress-induced crack propagation in another direction. By contrast, in the case of the RRM, the expansion stress uniformly accumulated around the reaction rim and the crack direction could be modified to the restraint direction even though the prior direction of expansion crack under free expansion was inhibited due to restraint stress. This may be an important factor that decides whether expansion transfer occurs.

The previous study by the authors [10] suggested that the GPM can explain the crack pattern of heterogeneous aggregates, such as those with a schistosity characteristic, and the RRM can explain the crack pattern of homogeneous aggregates, such as andesite. According to Sanchez et al. [9], this difference in the crack pattern was categorized by sharp crack and onion skin crack. The analytical results indicate that the aggregate type is determined by the internal crack pattern of the aggregates, and the difference in crack patterns probably causes macroscopic expansion under the restraint condition. Thus, the anisotropy of expansion may strongly depend on the difference in the internal crack patterns because the expansion pressure model and expansive site model are different. These analytical results indicate the possibility that the existence of expansion transfer depends on the difference in the distribution of the expansive site caused by the type of aggregates.

5. CONCLUSION

In this study, the effect of different distributions of the expansive sites inside aggregates on the anisotropy of expansion under stress was investigated by mesoscale discrete analysis. The findings are listed as follows:

1) The analytical modeling for the time-dependent behavior of ASR expansion was developed by the expansion pressure model (including the expansion stop model and crack effect model) to reproduce the plateau of the expansion. Furthermore, the coupling model with the expansion pressure model and expansive site model (i.e., the GPM and RRM) was proposed to investigate the effect of different distributions of the expansive sites inside aggregates on ASR expansion under stress. The analytical results confirmed that the ASR expansion behavior under a stress of less than 10 MPa can be reproduced.
2) The expansion stop model that describes the plateau of the expansion with the completion of the ASR reaction cannot reproduce the expansion transfer.
3) The crack effect model that describes the plateau of the expansion with the dissipation of expansion pressure due to the flow of the ASR gel into cracks induced by expansion can reproduce the expansion transfer in the case of the RRM.
4) With the GPM, expansion pressure locally accumulates at the expansive sites randomly distributed inside aggregates. The GPM cannot describe the expansion transfer for the following reason. The direction of crack propagation is fixed in advance owing to the arrangement of expansive sites, which prevents the propagation of cracks in another direction due to restraint stress.
5) With the RRM, expansion pressure uniformly distributes around the inner area of the reaction rim. The RRM can describe the expansion transfer owing to the following reason. The expansion stress uniformly accumulates around the reaction rim and the crack propagation direction can be modified according to the loading direction even though the prior direction of cracks under free expansion is inhibited perpendicular to the loading direction.
6) These analytical results indicate the possibility that the existence of expansion transfer depends on the different distributions of expansive sites due to the aggregates, and the aggregates can be the represented by the numerical tool.

References

[1] Rajabipour F, Giannini E, Dunant C, Ideker JH, Thomas MDA (2015) Alkali-silica reaction: current understanding of the reaction mechanisms and the knowledge gaps. Cem. Concr. Res. 76:130-146.

[2] Shi Z, Geng G, Leemann A, Lothenbach B (2019) Synthesis, characterization, and water uptake property of alkali-silica reaction products. Cem. Concr. Res. 121:58-71.

[3] Ichikawa T, Miura M (2007) Modified model of alkali-silica reaction. Cem. Concr. Res. 37:1291-1297.

[4] Kawabata Y, Dunant C, Yamada K, Scrivener K (2019) Impact of temperature on expansive behavior of concrete with a highly reactive andesite due to the alkali silica reaction. Cem. Concr. Res. 125. https://doi.org/10.1016/j.cemconres.2019.105888

[5] Multon S, Toutlemonde F (2006) Effect of applied stresses on alkali–silica reaction-induced expansions. Cem. Concr. Res. 36:912-920.

[6] Gautam BP, Panesar DK, Sheikh SA, Vecchio FJ (2017) Multiaxial expansion-stress relationship for alkali silica reaction-affected concrete, ACI Materials Journal 114-M17:171-184.[7] Dunant C, Scrivener KL (2010) Micro-mechanical modeling of alkali-silica-reaction induced degradation using the AMIE framework. Cem. Concr. Res. 40:517-525.

[8] Hansen SG, Hoang LC (2021) Anisotropic Compressive Behaviour of Concrete from Slabs Damaged by Alkali-Silica Reaction. Constr. Build. Mater. 267. https://doi.org/10.1016/j.conbuildmat.2020.120377

[9] Sanchez LFM, Fournier B, Jolin M, Duchesne J (2015) Reliable quantification of AAR damage through assessment of the Damage Rating Index (DRI). Cem. Concr. Res. 67:74-92.

[10] Miura T, Multon S, Kawabata Y (2021) Influence of the distribution of expansive sites in aggregates on microscopic damage caused by alkali-silica reaction: Insights into the mechanical origin of expansion. Cem. Concr. Res.142. https://doi.org/10.1016/j.cemconres.2021.106355

[11] Kawai T (1978) New discrete models and their application to seismic response analysis of structure. Nucl. Eng. Des. 48:207-229.

[12] Japan Society of Civil Engineers (2017) Standard Specifications for Concrete Structures – Design, Japan